

Wavefield Reconstruction Using a Whole Space Green's Function Framework

P. Terenghi* (PGS)

Summary

A whole-space Green's function framework for the representation of the acoustic wavefield is obtained from the Helmholtz wave equation. Under this framework, the wavefield is represented by a distribution of point-sources in space and time, each corresponding to an elementary spherical wavefront.

Intuition suggests the number of equivalent point sources actually required to represent the wavefield of interest might be small compared to the total number of speculative locations. Consequently, in spite of the problem's innate ill conditioned nature, a satisfying solution can still be obtained by means of sparsity promotion. When a solution is reached, the wavefield can be reconstructed at new or existing locations by utilizing the framework in a forward modelling sense.

Introduction

Coarse crossline sampling is certainly one of the limitations of towed marine acquisition. Streamers simply cannot be towed close enough to each other so as to produce wavefield measurements free of crossline aliasing. In the presence of significant scattering outside the survey plane, dense sampling in all directions (crossline as well as inline) becomes a theoretical requirement for several processing algorithms applied within individual shot experiments, such as up/down wavefield decomposition and wave-equation multiple prediction. Clearly, if crossline sampling requirements are to be satisfied, wavefield reconstruction must be able to operate well beyond the limits dictated by classical sampling theory.

Many established approaches to wavefield reconstruction use plane waves as their elementary basis functions. This choice is the origin of their need to work in small sliding data windows, especially in the presence of curvature in the time-offset domain. This requirement can constitute a limitation for applications such as crossline interpolation, where input is so sparsely sampled that it becomes impossible to conciliate two conflicting necessities: (1) to partition the data such that curvature is negligible, and (2) to ensure a sufficient number of input traces is fed to the reconstruction algorithm in each window.

At the scale of the observations that is characteristic of exploration seismology, spherical waves seem better suitable to represent seismic data than plane waves, as each spherical wavefront captures information distributed over the entire offset range, without requiring local sliding windows. As shown in the next section, the framework representing the proposed spherical decomposition in an acoustic context can be derived directly from the Helmholtz wave equation.

Theory

The linearity of the wave equation guarantees the wavefield P resulting from the ignition of a multiplicity of sources distributed across a given medium (of arbitrary complexity) always amounts to the sum of the wavefields G produced by elementary point-sources in the same medium (i.e. G is the medium's Green's function)

$$P(\omega, \mathbf{r}) = \int d\mathbf{r}' \rho(\omega, \mathbf{r}') G(\omega, \mathbf{r} - \mathbf{r}') \quad (\text{eq. 1}).$$

In (1), ω is the angular frequency, $\mathbf{r} = \{x, y, z\}$ the location of a generic receiver sensor (e.g. mounted on the seismic streamer) and $\mathbf{r}' = \{x', y', z'\}$ the generic location of an elementary point source in the spatial and temporal distribution ρ . Through the perturbative construct utilized in Inverse Scattering literature (Weglein et al., 1981 and references therein), (1) is generalized as

$$P(\omega, \mathbf{r}) = \int d\mathbf{r}' \rho_\alpha(\omega, \mathbf{r}') G_0(\omega, \mathbf{r} - \mathbf{r}') \quad (\text{eq. 2}),$$

where G_0 is the Green's function for a reference constant medium (e.g a whole or half space) with velocity c_0 . The role of ρ_α in (2) has changed remarkably with respect to the role of ρ in (1): ρ_α now represents a distribution of point-sources which can effectively produce, in a constant reference medium, the same wavefield P as the physical source produces in the complex medium. ρ_α can therefore be seen as a scattering potential (Weglein et al., 2003) responsible for all scattering phenomena. Because a whole-space Green's function is indeed an elementary spherical wavefront, (2) represents a spherical wave decomposition of the acoustic wavefield P .

It is further possible to define an augmented decomposition,

$$P(\omega, \mathbf{r}) = \sum_i \int d\mathbf{r}' \rho_\alpha(\omega, \mathbf{r}', c_i) G_0(\omega, \mathbf{r} - \mathbf{r}', c_i) \quad (\text{eq. 3}),$$

where the background velocity is also used as a spectral variable. In this case, although G_0 still represents a whole-space Green's function,

$$G_0(\omega, \mathbf{r} - \mathbf{r}', c) = \frac{e^{-i\frac{\omega}{c}|\mathbf{r}-\mathbf{r}'|}}{|\mathbf{r} - \mathbf{r}'|},$$

the single reference medium is replaced by a multiplicity of reference media. Although the additional degree of freedom can be seen as physically redundant, it is intuitive to realize that it allows each individual hyperbolic event in P to be mapped into a single equivalent source.

Numerically estimating ρ_α can be a daunting task as, in absence of prior information, the equivalent source responsible for a particular event might reside anywhere in 3-dimensional space and time, resulting in a massively underdetermined numerical inversion problem. Crucially, the Green's function framework described possesses the compressive characteristics required to work in combination with sparsity promoting solvers. As shown further in this document, early numerical tests conducted on real and synthetic datasets prove that satisfactory reconstruction of the seismic wavefield is possible well beyond the limits dictated by classical sampling theory.

As formulated, the proposed wavefield reconstruction method displays similarities with diffraction imaging and earthquake monitoring (McMechan, 1982; Chambers et al., 2009; Artman et al., 2010). Specifically, ray-traced and full-waveform Green's functions have been used in a compressive sensing context for the simultaneous determination of location, timing and moment tensor of natural and induced earthquakes (Vera Rodriguez et al., 2012; Vera Rodriguez and Sacchi, 2014). In contrast to all these methods, the described approach does not attempt to account for the wavefield's actual propagation history and does not require prior knowledge of the medium.

After all integrals are discretized, expression (3) can be cast into a linear system of the form $\mathbf{d} = \mathbf{L}\mathbf{m}$: the elements of P are arranged to populate vector \mathbf{d} , the element of ρ_α to populate vector \mathbf{m} and the columns of L are filled with different realizations of the whole-space Green's function G_0 , each characterized by an equivalent source location \mathbf{r}' , timing and background velocity. A solution is sought for applying a numerical solver that seeks to fit the data \mathbf{d} while minimizing the number of nonzero coefficients in \mathbf{m} . When a satisfying solution is reached, the wavefield can be reconstructed at new or existing locations by utilizing (3) as a forward modelling expression.

Examples

Finite difference synthetics. A first numerical example is conducted on a set of synthetic finite-difference data, simulated in a dipping plane reflector model. The wavefield is uniformly sampled with a trace spacing of 20.0m in the offset range between -2500 and 2500m (Figure 1b) and conditioned to contain temporal frequencies up to approximately 30Hz (Figure 1f). The wavefield is then uniformly under-sampled by a factor of 10 to form the input dataset (Figure 1a) with a trace spacing of 200m, where temporal frequencies above 3.75Hz are spatially aliased (Figure 1e). In this example, spectral estimation is conducted using an iteratively re-weighted least squares scheme, where anti-aliasing weights are obtained from low frequencies. The reconstructed wavefield and its FK spectrum are displayed in Figure 1c and Figure 1g, where aliasing has been resolved well beyond the constraints set by classical sampling theory.

Real data. The reconstruction scheme is further tested on the near offset portion (130 to 1000m) of a proximal streamer taken from a North Sea shot gather. The fully sampled data (70 traces with an offset interval of 12.5m) display significant frequency content up to roughly 110Hz (Figure 2a). Uniform under-sampling by a factor of 10, leads to a heavily aliased input dataset composed of 7 traces, mutually distanced by 125m (Figure 2b). The reconstructed result in Figure 2c (obtained using an anti-leakage matching pursuit solver) appears to be of satisfactory quality, considering the distance between input traces and the bandwidth of the signal. As expected, the magnitude of the reconstruction error (Figure 2d) is small in correspondence with available input traces and higher otherwise.

Conclusions

Wavefield reconstruction is pursued by promoting a sparse representation of the available measurements under a whole space Green's function framework. The framework itself can be derived from the Helmholtz equation and is therefore specific to seismic wavefields.

Numerical tests conducted on real and synthetic datasets prove that satisfactory reconstruction is achievable well beyond the limits dictated by classical sampling theory. Additionally, the method under consideration does not require prior knowledge of the earth's velocities.

Acknowledgement

PGS is gratefully acknowledged for providing the opportunity to investigate and permission to publish on this topic.

References

- Artman, B., Podladtchikov, I., and Witten, B. [2010] *Source location using time-reverse imaging*. *Geophysical Journal International*, 58, 861–873.
- Chambers, K., Kendall, J.M., Brandsberg-Dahl, S., and Rueda, J. [2009] *Testing the ability of surface arrays to monitor microseismic activity*. *Geophysical Prospecting*, 58, 821–830.
- McMechan, G.A., [1982] *Determination of source parameters by wavefield extrapolation*. *Geophys. J. R. astr. SOC.* 71, 613–628.
- Weglein, A.B., Boyse, W.E., and Anderson, J.E. [1981] *Obtaining 3-dimensional velocity information directly from reflection seismic data: An inverse scattering formalism*. *Geophysics* 46 (8), P1116–1120.
- Weglein, A. B., Araújo, F. V., Carvalho, P. M., Stolt, R. H., Matson, K. H., Coates, R. T., Corrigan, D., Foster, D. J., Shaw, S. A., and Zhang, H. [2003] *Inverse scattering series and seismic exploration*. *Inverse Problems*, 19(6), R27–R83.
- Vera Rodriguez, I., Sacchi, M.D., and Gu, Y.J. [2012] *A compressive sensing framework for seismic source parameter estimation*. *Geophysical Journal International*, 191, 1226–1236.
- Vera Rodriguez, I., and Sacchi, M.D. [2014] *Microseismic source imaging in a compressed domain*. *Geophysical Journal International*, 191, 1226–1236.

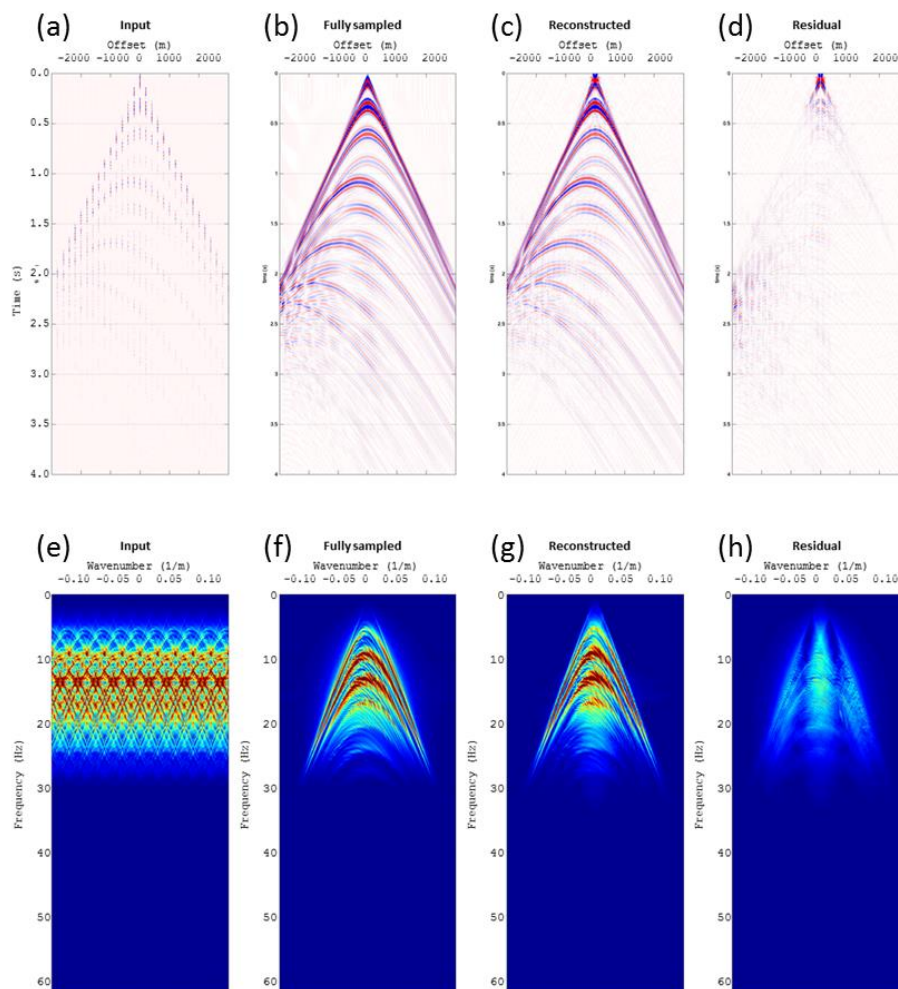


Figure 1 - Synthetic example. (a) Input data, (b) true wavefield, (c) reconstructed wavefield, (d) difference. FK spectra of (e) input data, (f) true wavefield, (g) reconstructed wavefield, (h) difference.

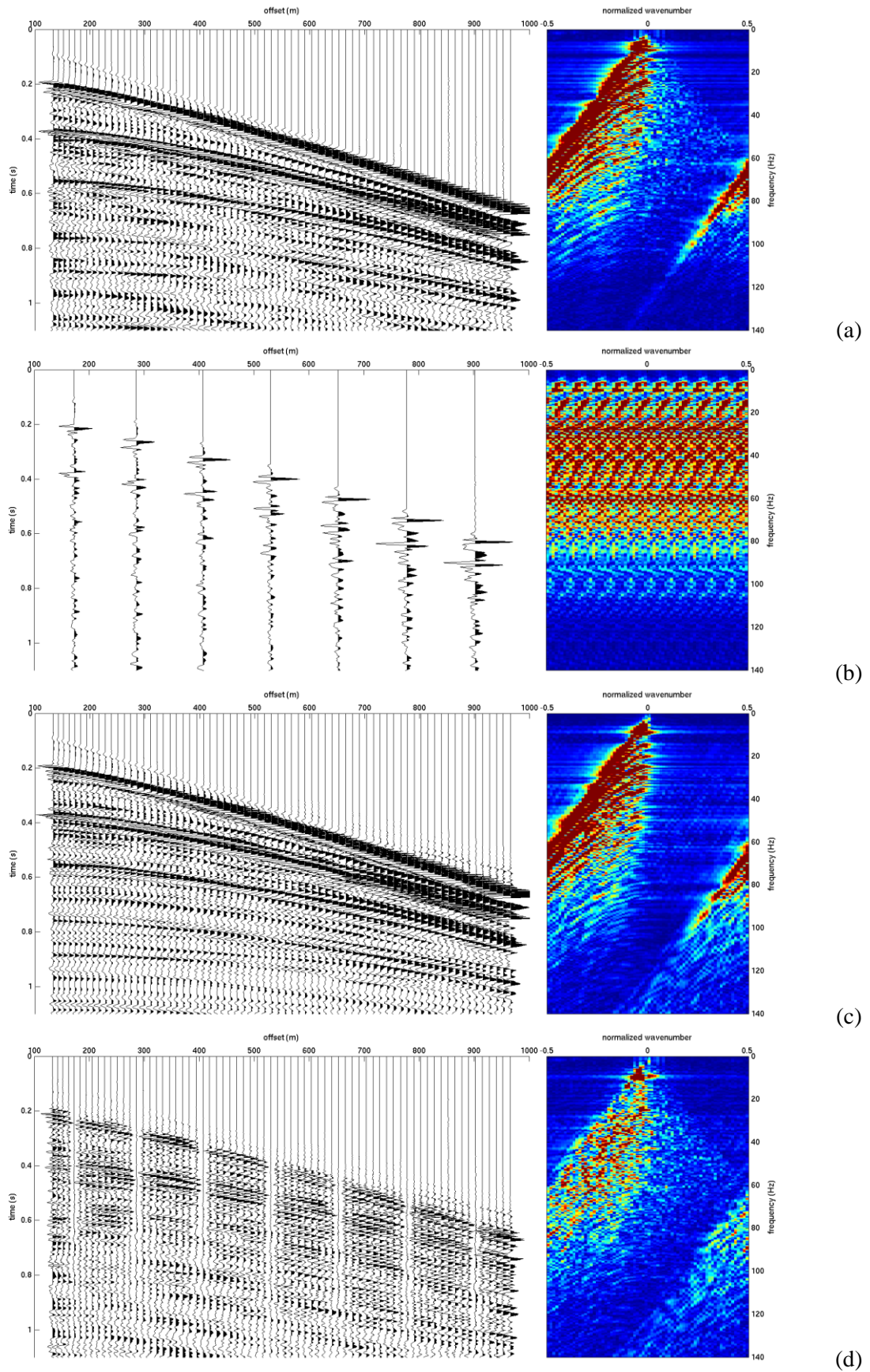


Figure 2 - North Sea example. Trace plots and FK spectra of (a) the fully sampled dataset with a trace spacing of 12.5m, (b) decimated dataset with a trace spacing of 125m, (c) the reconstructed dataset with a trace spacing of 12.5m obtained using data in (b) as input, (d) the reconstruction error.